Journal of Applied Sciences

ISSN 1812-5654

science alert

ANSInet
an open access publisher
http://ansinet.com

Journal of Applied Sciences 9 (13): 2362-2371, 2009
ISSN 1812-5654

Dynamic Assessment of Constrained Rigid Equipments

V. Sharif, M. Ghafory Ashtiany, S. Eshghi and A. Soroushian
International Institute of Earthquake Engineering and Seismology, P.O. Box 19395-3913, Tehran, Iran

Abstract: In this study, the dynamic behaviors of rigid constrained equipments under the harmonic excitations have been studied and analytical rocking response formulations have been introduced. Derived response formulations showed that the constraining of a rocking equipment by a link element can produce four different sets of response equations depending on the link stiffness and the place of link assembly. Buildup-like, beating-like and chaotic behaviors are some new aspects of the response in such equipments. Sensitivity analysis results showed that although in the most cases interning of the link element reduces the rocking response rotations but can increase the total damped energy during the contacts of the equipments to the base. This can be known as a risk for the equipments with leakage potential or with fragile wedges.

Key words: Rigid equipments, rocking, rigid block, simplifications, analytical response formulation

INTRODUCTION

Past earthquake reconnaissance studies showed that the toppling of the nonstructural components is the most commonly-seen damages in the buildings and industrial facilities (Anagnos, 2001). Direct and indirect losses caused by toppling of the rigid electric transformers during Northridge earthquake in 1994 emphasized the need for more studies about the dynamic behavior of these kinds of equipments to the organizations such as United States Pacific Gas and Electric Company (PG and E). Toppling of the rigid nonstructural components in the buildings also encouraged researchers for more studies in this field in a same manner (Singh *et al*., 2006). In dynamic assessment of the rigid equipments and nonstructural components, application of a model which is comprised of a rigid block under harmonic excitations can be seen widely in the past studies. Ishiyama (1982) concluded that the harmonic excitation can produce a good measure of the required condition for the toppling of the rocking block under the real earthquakes. Makris and Roussos (2000) also verified the application of the harmonic pulses as the representatives of the near-field pulse-like earthquakes. They finally concluded a reasonable accuracy in the application of harmonic excitation instead of the real earthquakes. Study about rocking behavior of a rigid block (Fig. 1) on a rigid base has been an interesting subject in past decades. Analytical solution of such system under harmonic excitation first was addressed by Housner (1963). The studies that followed Housner research can be categorized into some distinct

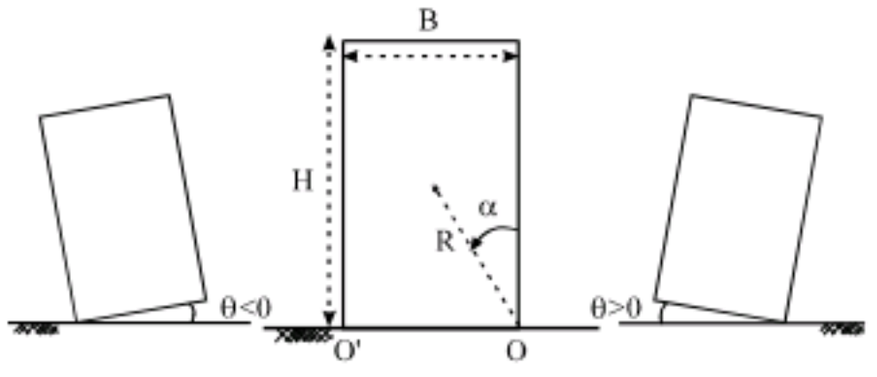

Fig. 1: Model of rigid block on a rigid base

areas: improving analytical formulations (Aslam *et al*., 1980; Spanos and Koh, 1984; Makris and Roussos, 2000), incorporating the other modes of response such as sliding mode in the rocking response formulations (Shenton and Jones, 1991a, b; Yang *et al*., 2000), considering the chaotic behavior of a rocking block (Hogan, 1994, 1990, 2000; Yim and Lin, 1991; Jeong *et al*., 2003), comparison of the analytical and experimental results (Tso and Wong, 1989; Wong and Tso, 1989; Peña *et al*., 2007), incorporating the base flexibility (Psycharis, 1981), using real or generated seismic excitations instead of harmonic excitations (Yim *et al*., 1980; Apostolou *et al*., 2007; Boroschek and Iruretagoyena, 2006). Further researches focused on the effects of anchor bolts and interaction issues on the final rocking response of the equipments (Der-Kiureghian, 1999; Makris and Zhang, 1999). Makris and Zhang (1999) showed that anchoring of an equipment to the base does not essentially lead to a safer equipment against toppling under seismic excitation. In the study of Makris and Zhang (1999), a model composed of a rigid block standing on a rigid base which is connected to the

Corresponding Author: Vahid Sharif, International Institute of Earthquake Engineering and Seismology, No. 26 Arghavan Street, North Dibaji Avenue, P.O. Box 19395-3913, Tehran, Iran
Tel: +98 21 2283116-19/454, +98 912 3342922 Fax: +98 21 55388750

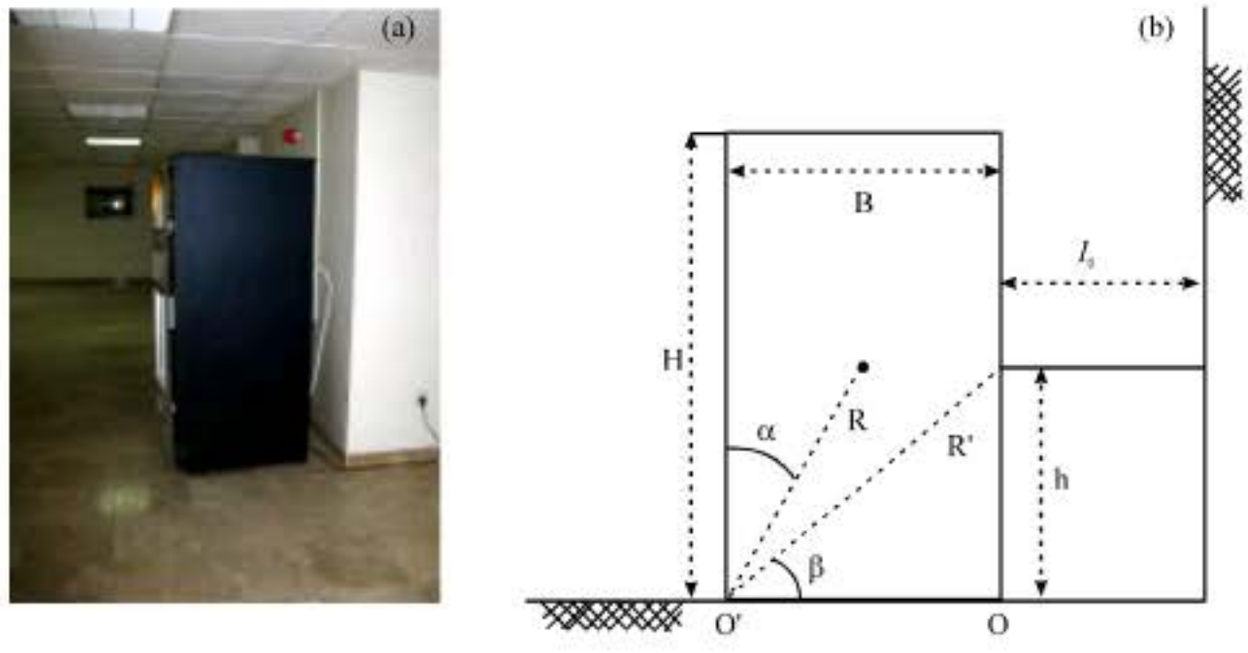

Fig. 2: (a) An automatic vendor machine (constrained rigid equipment) and (b) mathematical model of constrained rigid equipment

base by ductile or brittle anchors has been used in analysis. In a related study, Der-Kiureghian (1999) showed that interconnection between two electrical transformers can amplify the response of the stiffer equipment and de-amplify the response of the softer equipment. In Der-Kiureghian (1999) study, two Single Degree of Freedom (SDOF) systems as the representatives of substation transformers have been used. In this study, the analytical rocking response formulations of a rigid equipment which stands on a rigid base (e.g., rigid floor) and is connected with a flexible connection (e.g., pipes) to a supporting structure (e.g., wall) under harmonic excitation have been introduced. Such system (Constrained equipments) can be modeled in the simplest form by a rigid block on a rigid base which connected with a spring to a supporting structure. Figure 2a and b show the model which has been used in this research. The assumptions of this study are: friction is large enough to avoid sliding of the block, the base excitation is harmonic and link element has been assembled parallel to the base.

ANALYTICAL RESPONSE DERIVATION OF FREE-STANDING EQUIPMENTS

The governing rocking equations of a free-standing rigid block on a rigid base can be written as follow (Fig. 1):

$$I\ddot{\theta} = -MgR\sin(\alpha-\theta) - M\ddot{u}_g R\cos(\alpha-\theta) \qquad \theta>0 \qquad (1a)$$

$$I\ddot{\theta} = +MgR\sin(\alpha+\theta) - M\ddot{u}_g R\cos(\alpha+\theta) \qquad \theta<0 \qquad (1b)$$

where, M is the mass of block, g is gravity acceleration, $\ddot{u}_g$ is horizontal base acceleration, R is the radius of block and α is critical angle as shown in Fig. 1 and I is block moments of inertia about block corners (in a rectangular block $I = 4/3\ MR^2$). The sign of θ is positive when the block rotates about its right corner and it is negative when it rotates about its left corner (Fig. 1).

The Eq. 1a and b do not have easy-to-be-derived closed-form solution; therefore some simplifying assumptions are required for converting the original Eq. 1a and b into the simpler forms. Housner (1963) used assumptions as follow for slender blocks ($B/H = \tan(\alpha) \approx \alpha$):

$$\begin{aligned}&\cos(\alpha\pm\theta)\cong 1\\ &\sin(\alpha\pm\theta)\cong \alpha\pm\theta\end{aligned} \qquad (2)$$

Using Eq. 2 and dividing two sides of the Eq. 1a and b onto the block moment of inertia (I) and assuming, $\ddot{u}_g = a_p \sin(\omega t+\Psi)$ as the ground motion, the simplified governing equations become:

$$\ddot{\theta} - p^2\theta = -\frac{a_p}{g}\sin(\omega t+\psi)p^2 - p^2\alpha \qquad \theta>0 \qquad (3a)$$

$$\ddot{\theta} - p^2\theta = \frac{a_p}{g}\sin(\omega t+\psi)p^2 + p^2\alpha \qquad \theta<0 \qquad (3b)$$

Where:

$$\begin{aligned}p &= \sqrt{3g/4R}\\ \psi &= \sin^{-1}(\alpha g/a_p)\end{aligned} \qquad (4)$$

The simplified Eq. 3a and b have the analytical solutions as follow:

$$\theta = A_1\sinh(pt) + A_2\cosh(pt) + \alpha + \frac{1}{1+\frac{\omega^2}{p^2}}\frac{a_p}{g}\sin(\omega t+\psi) \qquad \theta>0 \qquad (5a)$$

$$\theta = A_3 \sinh(pt) + A_4 \cosh(pt) - \alpha + \frac{1}{1+\frac{\omega^2}{p^2}} \frac{a_p}{g} \sin(\omega t + \psi) \quad \theta < 0 \tag{5b}$$

where, constants of A_1 to A_4 can be calculated by incorporation of the initial conditions as follow:

$$A_1 = A_3 = \frac{\dot{\theta}_0}{p} - \frac{\frac{\omega}{p}}{1+\frac{\omega^2}{p^2}} \frac{a_p}{g} \cos(\psi)$$
$$A_{2,4} = \theta_0 \pm \alpha - \frac{1}{1+\frac{\omega^2}{p^2}} \frac{a_p}{g} \sin(\psi) \tag{6}$$

where, θ_0 and $\dot{\theta}_0$ are the initial rotation and angular velocity of the block, respectively. After each contact of the block to the base, the contact velocity will be reduced by a restitution factor (ν). The restitution factor can be defined and calculated as Ishiyama (1982):

$$\nu = \dot{\theta}^{after} / \dot{\theta}^{before}$$
$$\nu = 1 - 3/2(\sin(\alpha))^2 \tag{7}$$

where, $\dot{\theta}^{before}$ and $\dot{\theta}^{after}$ imply to the angular velocity of the block before and after contact, respectively. The after-contact velocity ($\dot{\theta}^{after}$) will be used as initial condition for the governing equations of the opposite direction.

Using Eq. 5a and b, Housner (1963) derived minimum required amplitude of a half-sine and full-sin pulse for the toppling of a rigid block (toppling condition is $|\theta| \geq \alpha$).

CONSTRAINED EQUIPMENTS RESPONSE DERIVATIONS

Figure 2a shows a sample of constrained equipment which is an automatic vendor machine that connected by a flexible pipe to the wall. Figure 2b shows its appropriate mathematical model. Here, first the exact rocking governing equations of the constrained equipments have been introduced. Later, the suitable numerical schemes for solving these equations are addressed. Following that, the analytical response formulations are derived using simplifying assumptions.

Exact governing equations: In derivation of the governing equations of the constrained equipments, as shown in Fig. 3, the moments due to the interacting force must be incorporated in the governing equations. It should be noted that the amount (f_i) and acting angle of the interaction force (γ) and its acting arm (NAA, IAA), as shown in Fig. 3, change simultaneously with the block rotation.

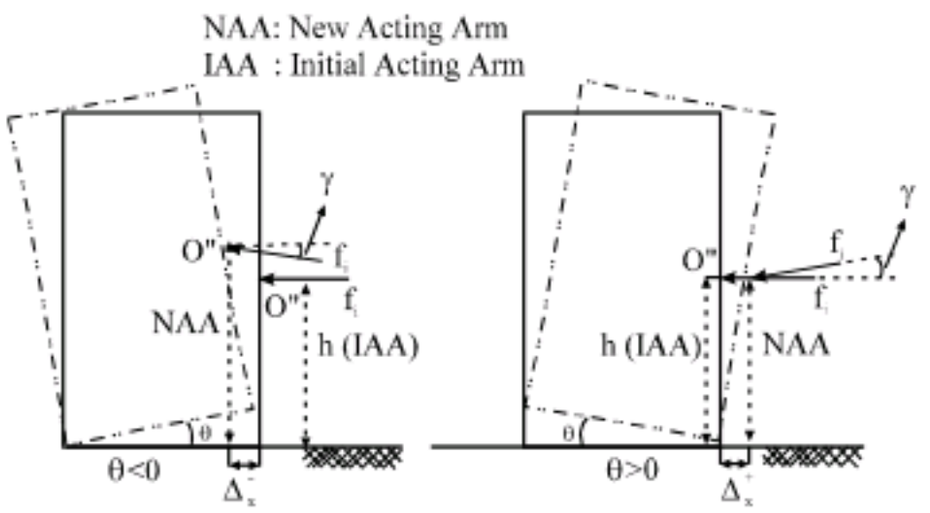

Fig. 3: Changes of ink force acting arm (NAA, IAA) and acting angle (γ) with block rotation

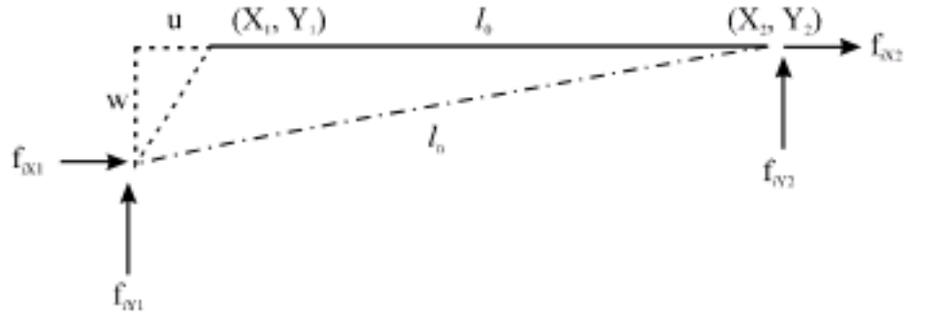

Fig. 4: Link element forces and displacements

Table 1: Formulation of Nodal displacement of link element

Displacement of O"	θ>0	θ<0
u	$l \sin(\theta)$	$R' \cos(\beta-\theta)-B$
w	$l (\cos(\theta)-1)$	$R' \sin(\beta-\theta)-B$

Considering this matter that the interaction force amount is only function of deformed length of the link element, by calculation of this parameter, the moments due to the link force can be entered into the governing equations. The deformed length of the link element (l_n) can be calculated as follow:

$$l_n = \sqrt{\Delta_{LX}^2 + \Delta_{LY}^2} \tag{8}$$

Where:

$$\Delta_{LX} = X_2 - X_1 - u = l_0 - u$$
$$\Delta_{LY} = Y_2 - Y_1 - w = -w \tag{9}$$

In which, (X_1, Y_1), (X_2, Y_2) are initial coordinates of the connecting nodes of the link element, u, w are the nodal displacement of O" (Fig. 3) and can be calculated according to the Table 1, l_0 is the initial length of the link element as shown in Fig. 4.

Using the virtual work principle on the deformed shape of the link element (Fig. 4), one can write:

$$\delta E_P = k(l_n - l_0)\delta l_n$$
$$\delta E_E = f_{iX1}\delta u_1 + f_{iY1}\delta w_1$$
$$\delta E_E = \delta E_P \tag{10}$$

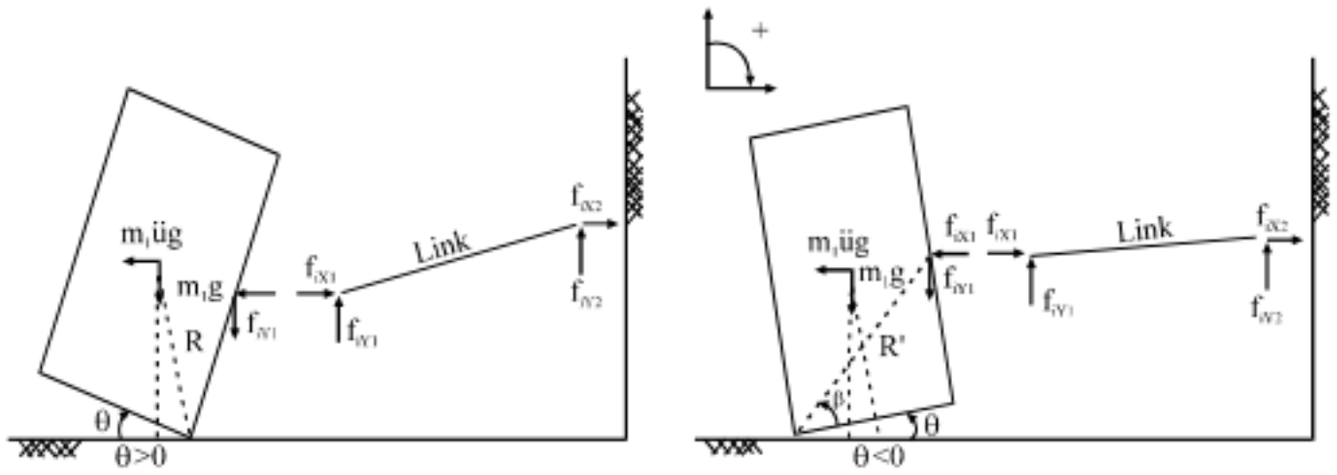

Fig. 5: Free body diagram of a constrained rigid block including vertical and horizontal components of link force

where, δE_P is the change in potential energy and δE_E is the virtual works done by link forces. In Eq. 10, the parameter of δl_n can be calculated as follow:

$$\begin{aligned}\delta l_n &= \frac{\partial l_n}{\partial u_1}\delta u_1 + \frac{\partial l_n}{\partial w_1}\delta w_1\\ \frac{\partial l_n}{\partial u_1} &= \frac{-\Delta_{LX}}{l_n}\\ \frac{\partial l_n}{\partial w_1} &= \frac{-\Delta_{LY}}{l_n}\end{aligned} \tag{11}$$

Consequently the link forces in arbitrary time of t become:

$$f_{iX1} = -f_{iX2} = \left(\frac{-\Delta_{LX}}{l_n}\right)k(l_n - l_0) \tag{12a}$$

$$f_{iY1} = -f_{iY2} = \left(\frac{-\Delta_{LY}}{l_n}\right)k(l_n - l_0) \tag{12b}$$

where, k is the link stiffness.

Using Eq. 12, the rocking governing equations (Fig. 5) become:

$$I\ddot{\theta} = -MgR\sin(\alpha-\theta) - Ma_p\sin(\omega t+\psi)R\cos(\alpha-\theta) - f_{iX1}h\cos(\theta) + f_{iY1}h\sin(\theta) \qquad \theta > 0 \tag{13a}$$

$$I\ddot{\theta} = +MgR\sin(\alpha+\theta) - Ma_p\sin(\omega t+\psi)R\cos(\alpha+\theta) - f_{iX1}R'\sin(\beta-\theta) + f_{iY1}R'\cos(\beta-\theta) \qquad \theta < 0 \tag{13b}$$

where, R', h, β have been shown in Fig. 2b.

Differential Eq. 13 can be solved by means of numerical schemes. In this study the combination of Average Acceleration and Modified Newton Raphson has been used. This method recommended by Bathe (1996) in application of the implicit solvers in the nonlinear dynamics. In analysis process, the detection of the contact time of the block to the base is important. At this point, the governing equation switches from one set to another set of equation (for example Eq. 13a switches to Eq. 13b) and a locating event algorithm as had been addressed by Bernal (1991) is required. In this study, Fractional Time Stepping (Mahin and Lin 1983; Nau, 1983) has been used as the locating event finder algorithm. Whereas the detection of the exact contact time is not possible practically, this time should be detected with a prescribed accuracy. Allen and Duan (1995) assumed the $|\theta|<10^{-6}$ condition as criterion for detecting of the time where the block contacts to the base. In this research same criterion has been used.

Analytical derivations: Closed-form solution of the exact governing equations of the rocking motion (Eq. 13) is not easy to be derived; Therefore for derivation of the analytical solution, two assumptions have been used in this study as follow:

- The vertical component of the interaction force is negligible and block rotation (θ) is small. By this assumption, the moments (M_i) due to the interaction force (f_i) becomes:

$$M_i \cong f_i h \tag{14}$$

To obtain f_i as a function of θ, the displacements of the connecting node O" (Δx^+, Δx^-) as shown in Fig. 3 in arbitrary time of t should be calculated. From Fig. 2b and 3 one can write:

$$\begin{aligned}\Delta_X^+ &= h\sin(\theta)\\ \Delta_X^- &= R'\cos(\beta-\theta) - B \cong R'[\cos(\beta) + \theta\sin(\beta)] - B\end{aligned} \tag{15a}$$

$$\begin{aligned}R'\sin(\beta) &= h\\ R'\cos(\beta) &= B\end{aligned} \tag{15b}$$

where, Δx^+ and Δx^- are the displacement of node O" in the states of $\theta>0$ and $\theta<0$, respectively. Combination of Eq. 15a and b results to:

$$\Delta_X^- \cong \Delta_X^+ \cong h\theta = \Delta_X \tag{16}$$

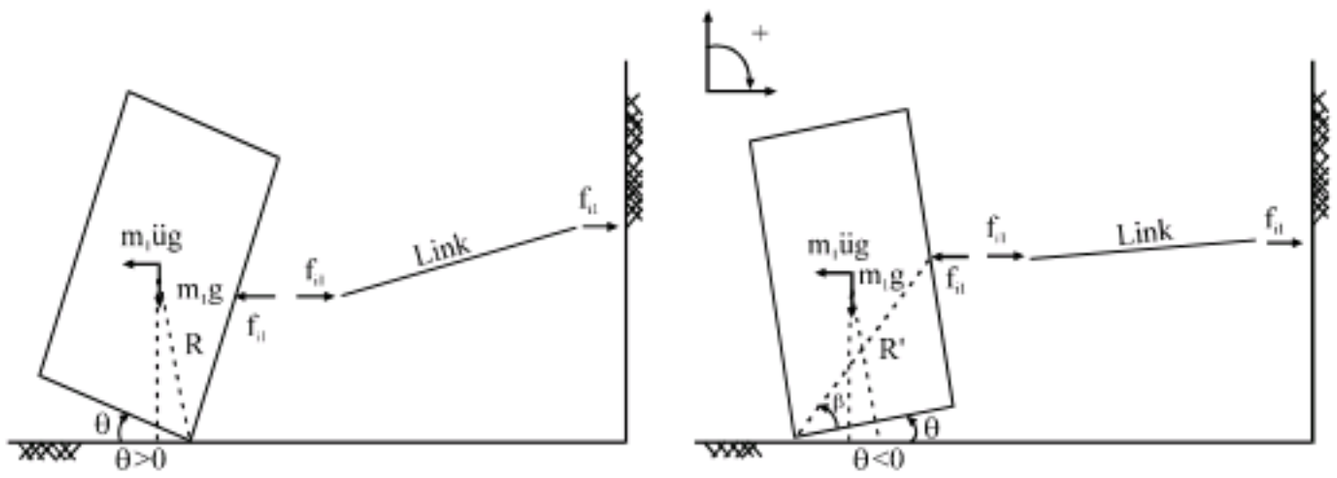

Fig. 6: Free body diagram of a constrained rigid block ignoring vertical component of link force

Using Eq. 16, the simplified forms of the interaction forces can be written as follow:

$$f_{i1} = -f_{i2} \cong k\Delta_x \cong kh\theta \quad (17)$$

- For small rocking motions of θ it can be assumed that:

$$\cos(\alpha \pm \theta) \cong \cos(\alpha) \quad (18a)$$

$$\sin(\alpha \pm \theta) \cong \sin(\alpha) \pm \theta\cos(\alpha) \quad (18b)$$

Using the first assumption (Eq. 17) and assuming $\ddot{u}_g = a_p \sin(\omega t+\Psi)$, the governing equations of the motion (Fig. 6) can be written as:

$$I\ddot{\theta} = -MgR\sin(\alpha-\theta) - Ma_p\sin(\omega t+\psi)R\cos(\alpha-\theta) - f_{i1}h \quad \theta>0 \quad (19a)$$

$$I\ddot{\theta} = +MgR\sin(\alpha+\theta) - Ma_p\sin(\omega t+\psi)R\cos(\alpha+\theta) - f_{i1}h \quad \theta<0 \quad (19b)$$

Using the second assumption (Eq. 18) and dividing two sides of Eq. 19 onto the block moment of inertia (I), the governing equations become:

$$\ddot{\theta} - (p'^2 - \frac{kh^2}{I})\theta = -\frac{a_g}{g}\sin(\omega t+\psi).p'^2 - p'^2\tan(\alpha) \quad \theta>0 \quad (20a)$$

$$\ddot{\theta} - (p'^2 - \frac{kh}{I})\theta = -\frac{a_g}{g}\sin(\omega t+\psi).p'^2 + p'^2\tan(\alpha) \quad \theta<0 \quad (20b)$$

where, $p' = p\sqrt{\cos(\alpha)}$ and p has been defined earlier in Eq. 3. Equation 20 has four sets of analytical solution depending on the sign of p'^2-kh^2/I and the excitation frequency (ω) as follow:

- State one, $q^2 = p'^2-kh^2/I>0$

$$\theta = A_1\sinh(qt) + A_2\cosh(qt) + \frac{p'^2}{q^2}\tan(\alpha) + \frac{p'^2}{\omega^2+q^2}.\frac{a_p}{g}\sin(\omega t+\psi) \quad \theta>0 \quad (21a)$$

$$\theta = A_3\sinh(qt) + A_4\cosh(qt) - \frac{p'^2}{q^2}\tan(\alpha) + \frac{p'^2}{\omega^2+q^2}.\frac{a_p}{g}\sin(\omega t+\psi) \quad \theta<0 \quad (21b)$$

where, constants of A_1 to A_4 can be calculated by incorporation of initial conditions as:

$$A_1 = A_3 = \frac{\dot{\theta}_0}{q} - \frac{p'^2}{\omega^2+q^2}.\frac{a_p}{g}.\frac{\omega}{q}\cos(\psi)$$
$$A_{2,4} = \theta_0 \mp \frac{p'^2}{q^2}\tan(\alpha) - \frac{p'^2}{\omega^2+q^2}.\frac{a_p}{g}\sin(\psi) \quad (22)$$

- State two and $-q^2 = p'^2-kh^2/I<0$ and $\omega \neq q$

$$\theta = A_1\sin(qt) + A_2\cos(qt) - \frac{p'^2}{q^2}\tan(\alpha) + \frac{p'^2}{\omega^2-q^2}.\frac{a_p}{g}\sin(\omega t+\psi) \quad \theta>0 \quad (23a)$$

$$\theta = A_3\sin(qt) + A_4\cos(qt) + \frac{p'^2}{q^2}\tan(\alpha) + \frac{p'^2}{\omega^2-q^2}.\frac{a_p}{g}\sin(\omega t+\psi) \quad \theta<0 \quad (23b)$$

Where:

$$A_1 = A_3 = \frac{\dot{\theta}_0}{q} - \frac{p'^2}{\omega^2-q^2}.\frac{a_p}{g}.\frac{\omega}{q}\cos(\psi)$$
$$A_{2,4} = \theta_0 \pm \frac{p'^2}{q^2}\tan(\alpha) - \frac{p'^2}{\omega^2-q^2}.\frac{a_p}{g}\sin(\psi) \quad (24)$$

- State three and $q^2 = p'^2-kh^2/I<0$ and $\omega = q$ (name it resonance state)

$$\theta = A_1\sin(qt) + A_2\cos(qt) + \frac{a_g}{2g}.\frac{p'^2}{q}t.\cos(\omega t+\psi) - \frac{p'^2}{q^2}\tan(\alpha) \quad \theta>0 \quad (25a)$$

$$\theta = A_3\sin(qt) + A_4\cos(qt) + \frac{a_g}{2g}.\frac{p'^2}{q}t.\cos(\omega t + \psi) + \frac{p'^2}{q^2}\tan(\alpha) \quad \theta < 0 \tag{25b}$$

Where:

$$A_1 = A_3 = \frac{\dot{\theta}_0}{q} - \frac{a_g}{2g}.\frac{p'^2}{q^2}\cos(\psi)$$
$$A_{2,4} = \theta_0 \pm \frac{p'^2}{q^2}\tan(\alpha) \tag{26}$$

- State four, $q^2 = p'^2 - kh^2/I = 0$ (denoting k by k_0 in this state)

$$\theta = \frac{a_g}{g\omega^2}\sin(\omega t + \psi)p'^2 - \frac{p'^2}{2}\tan(\alpha).t^2 + A_1 t + A_2 \quad \theta > 0 \tag{27a}$$

$$\theta = \frac{a_g}{g\omega^2}\sin(\omega t + \psi)p'^2 + \frac{p'^2}{2}\tan(\alpha).t^2 + A_3 t + A_4 \quad \theta < 0 \tag{27b}$$

Where:

$$A_1 = A_3 = \dot{\theta}_0 - \frac{a_g}{g\omega}\cos(\psi)p'^2$$
$$A_2 = A_4 = \theta_0 - \frac{a_g}{g\omega^2}\sin(\psi)p'^2 \tag{28}$$

By comparison of Eq. 21-28 with response formulations of the free-standing rocking block (Eq. 5 and 6), one can find that the interning of the link element can make different variants in the rocking response formulations. In addition to this variety, presence of periodic terms (e.g., state three) makes probable appearance of some new phenomenon such as resonance in the response space. In the following sections some case studies of these new aspects have been presented.

SPECIAL ASPECTS OF THE RESPONSE

Here, although vast analysis have been done and limited case studies have been presented (Table 2). In the selected case studies, the normalized rotation (θ/α) has been selected as the output parameter. The specifications of the case studies have been selected to proof some new response pattern possibility. As can be seen in Eq. 21, the formulation of the state one is same as free-standing block response formulation (Eq. 5 and 6) with this difference that only parameter of p changed to $q(q = \sqrt{p'^2 - kh^2/I})$ therefore same response behavior is expectable. As this state has been studied by many researchers in past decades, this study focused on presenting new cases (states two to four). In selected case studies, the excitation frequency (ω) and link stiffness (k) have been taken as factors (N and S) of the system parameter (q) and k_0 (state four for definition of k_0), respectively as follow:

$$\omega = N.q \qquad k = S.k_0 \tag{29}$$

For the state four where, S = 1, because $q^2 = p'^2 - kh^2/I = 0$ ($k = k_0$), the excitation frequency (ω) has been taken equal to p' and has been remarked as N/A in Table 2. Ground motion duration has been defined as the number of half-sin pulses. Figure 7 shows an excitation with four half-sin pulses. Whereas minimum base acceleration amplitude (a_p) for setting the block into the rocking motion is $a_p = (B/H).g$, the amplitude (a_p) has been selected from the values with $a_p > (B/H).g$ where, B and H have been shown in Fig. 2b. For examining the efficiency of analytical formulations, the numerical solutions of governing Eq. 13 have been calculated and plotted in the same figure with analytical results. In each case study, the maximum absolute error (err_a) according to Eq. 30 has been calculated and has been shown in Fig. 8-12. In calculation of the absolute error, the results obtained from Average

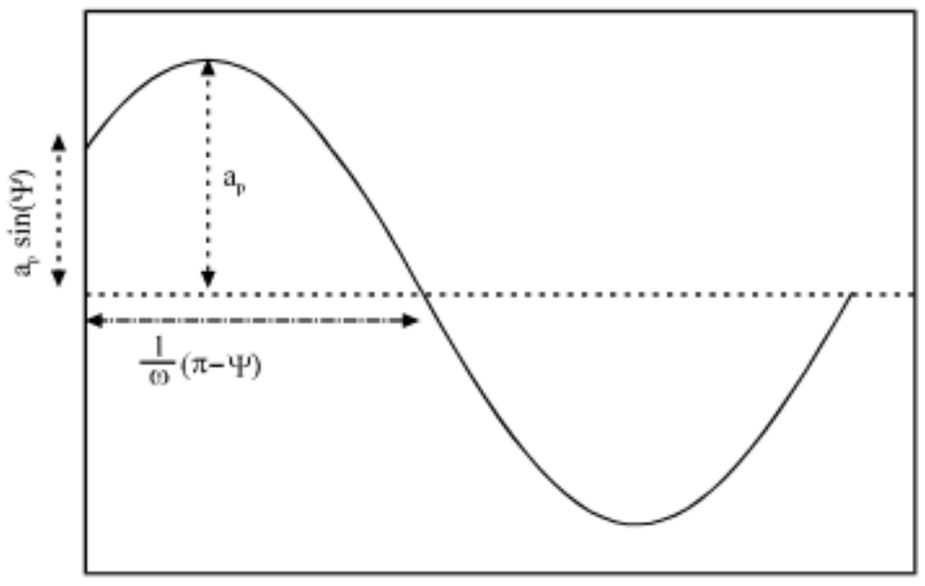

Fig. 7: Base excitation includes four half-sin pulses

Table 2: Case studies specification for presenting special aspect of response

Case study No.	B (m)	H (m)	h (m)	l_0 (m)	a_p (g)	S	N	No. of half-sin pulses	Appropriate figure
1	0.7	2.1	1.1	1.5	0.39	6	0.675	6	Fig. 8a
2	0.6	2.4	1.2	1.5	0.45	6	3.5	6	Fig. 8b
3	0.7	2.1	1.1	1.5	0.45	40	1	30	Fig. 9
4	0.6	2.4	1.2	1.5	0.31	5	1	80	Fig. 10
5	0.7	2.1	1.1	1.5	0.38	3	1	6	Fig. 11
6	0.6	2.4	1.2	1.5	0.27	1	N/A	6	Fig. 12

N/A: Not available

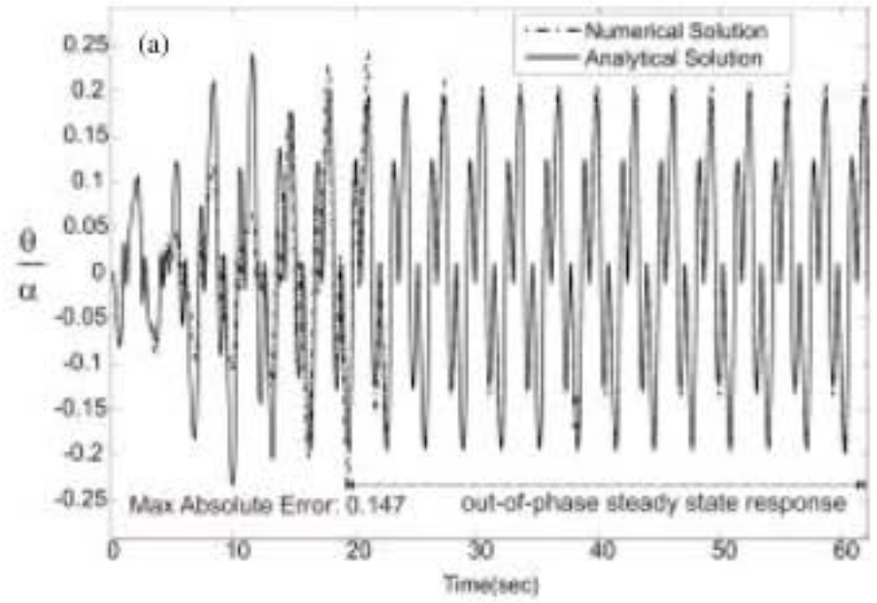

Fig. 8: Steady state rocking response: (a) case study No. 1 and (b) case study No. 2 according to Table 2

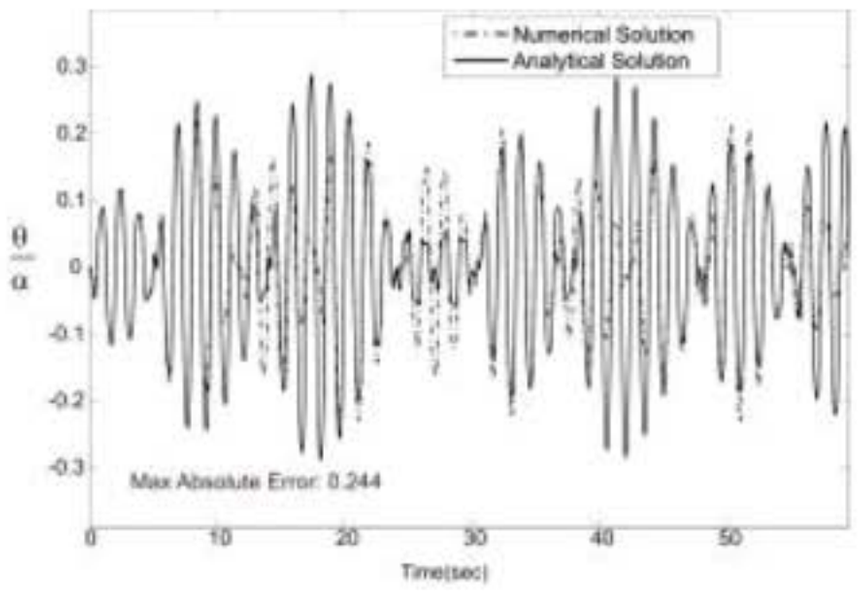

Fig. 9: Beating-like rocking response, case study No. 3 according to Table 2

acceleration method (N_s) have been taken as the exact solution and have been compared with analytical solutions (A_s):

$$err_s = Max\left\|N_s - A_s\right\| \quad (30)$$

One of the special aspects of the rocking response in the state two is the appearance of steady state rocking motion. Figure 8a and b shows asymmetric and symmetric

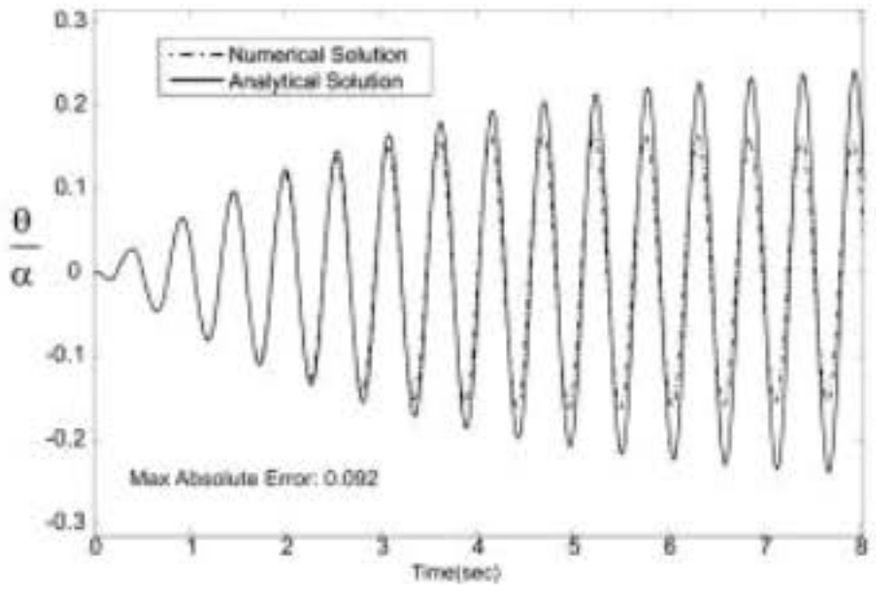

Fig. 10: Buildup-like rocking response, case study No. 4 according to Table 2

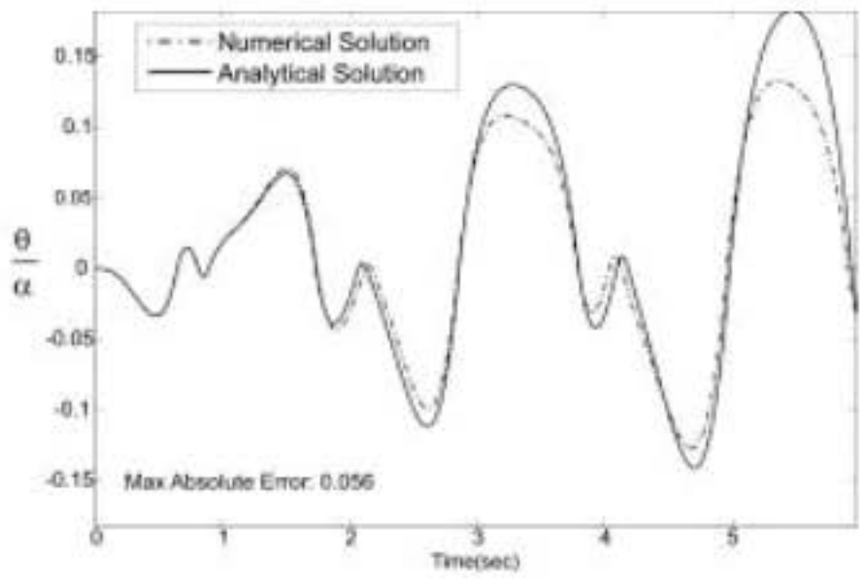

Fig. 11: Irregular (chaotic) rocking response, case study No. 5 according to Table 2

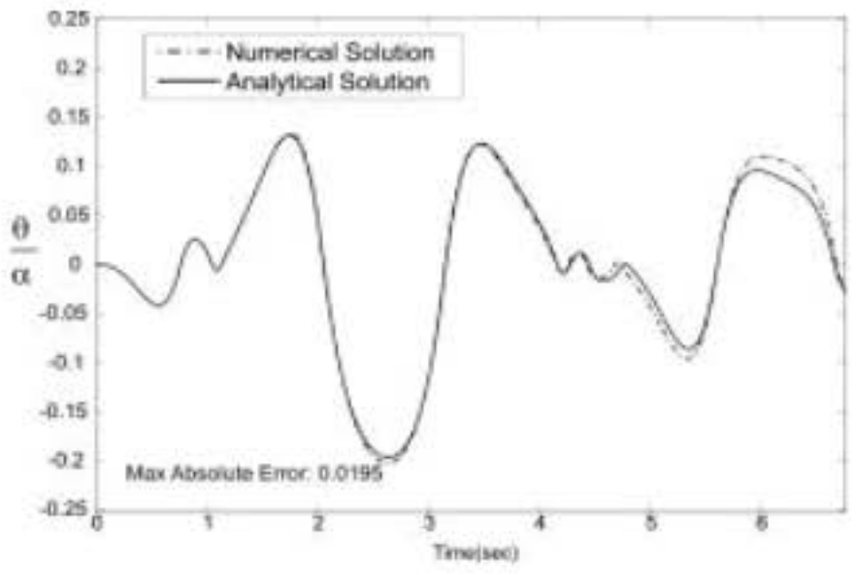

Fig. 12: Irregular (chaotic) rocking response, Case study No. 6 according to Table 2

out-of-phase steady state rocking motion, respectively (case study No. 1, 2 Table 2). The expression of out-of-phase as had been addressed by Tso and Wong (1989) indicates to a kind of response where after some unsteady cycles, the steady state response takes form. This kind of response also can be seen in free-standing rigid blocks (Hogan, 1990). Figure 9-11 shows some interesting

response patterns such as buildup-like, beating-like and irregular patterns respectively for the resonance state (S>1, N = 1). In spite of the resonance response of a SDOF system which has unique response pattern (buildup only), in the rocking response of a constrained block, three patterns can take form. Considering state four, Fig. 12 shows that the irregular (chaotic) behavior is the dominant pattern in this state.

SENSITIVITY ANALYSIS

The effects of the link element on the maximum normalized rotation of the rigid block (Max(|θ|)/α) in various excitation frequency (ω) have been studied. In this study a new parameter as the damage index (DMG) has been introduced. The damage index is the cumulative differences between kinetic energy before contacts (E_k^{before}) and after contacts (E_k^{after}) in the forced vibration phase. More damped energy (E_d) during the excitation can be interpreted as more damage to the equipments (e.g., damage to the wedge of equipments even if they do not topple). The damage index accordingly can be formulated as:

$$DMG = \sum_{i=1}^{n}(E_d)_i = \sum_{i=1}^{n}(E_k^{before} - E_k^{after})_i = \sum_{i=1}^{n}\frac{1}{2}I(\dot{\theta}^{before})_i^2(1-\nu^2) \quad (31)$$

where, n is the No. of contacts of the block to the base. Because the analytical formulations derived by using some simplifying assumptions and calculation of the damage index according Eq. 31 may cumulate errors of such simplification n times, therefore some discrepancies between numerical and analytical approaches on the calculation of this parameter may be observed.

The case studies specifications have been shown in Table 3. In each case study, the constrained block has been analyzed under a periodic excitation that includes 4 half-sin pulse with a fixed amplitude (a_p, according Table 3) but with different frequencies (ω) which sweep a range from q/10 to 6q with the increments of q/10. In each analysis the maximum normalized rotation and damage index have been calculated and plotted against excitation frequencies. This procedure is shown in Fig. 13 schematically. For better understanding the effects of the link element on the final response of the constrained block, the maximum normalized rotation and damage index for free-standing state (same block but without link element) have been calculated and plotted. Figure 14 shows that in a wide range of excitation frequencies, the maximum normalized rotation has been reduced when it was compared with free-standing state. In some rare frequency ranges (frequency range that is marked as G in Fig. 16) the link element caused amplification of the

Table 3: Case studies specification for sensitivity analysis

Case study No.	B (m)	H (m)	h (m)	m (kg)	l_0 (m)	a_p (g)	k (N m^{-1})
1	0.7	2.1	0.525	200	1.5	0.533	50000
2	0.7	2.1	0.525	400	1.5	0.533	50000
3	0.6	2.4	1.200	200	1.5	0.450	50000

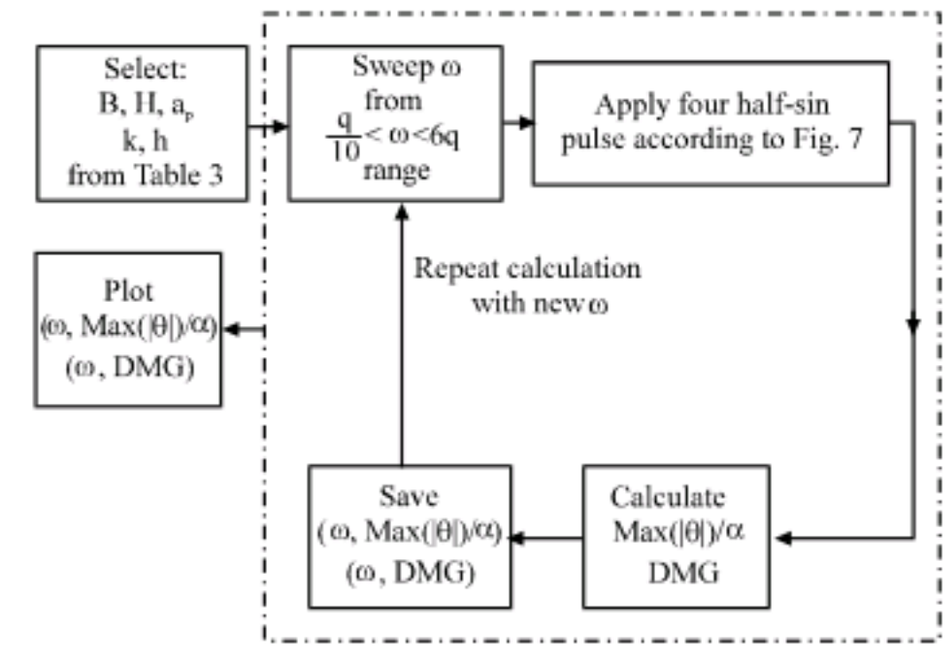

Fig. 13: Sensitivity analysis procedure

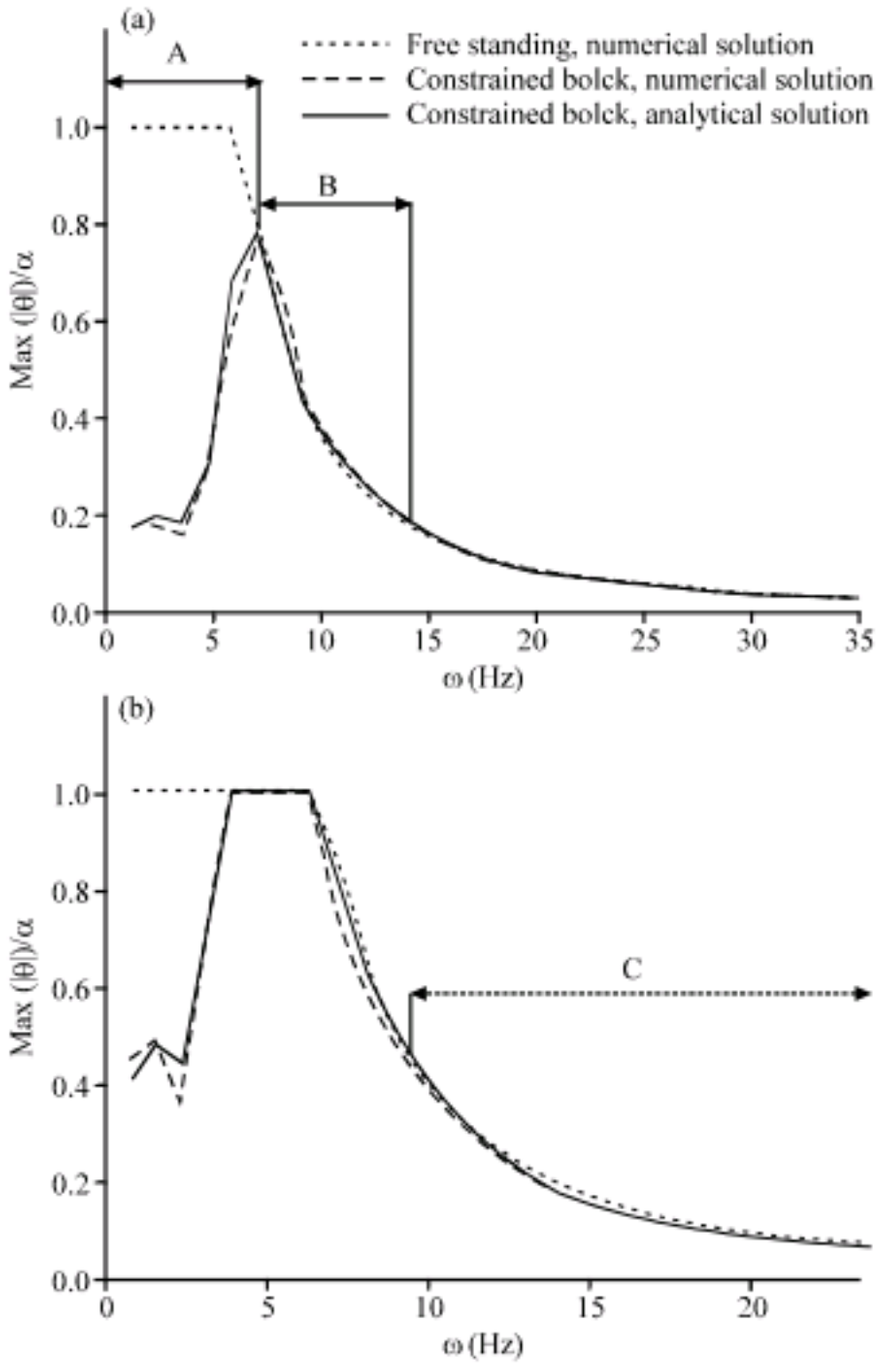

Fig. 14: Maximum normalized rocking response (a) case study No. 1 and (b) case study No. 2 according to Table 3

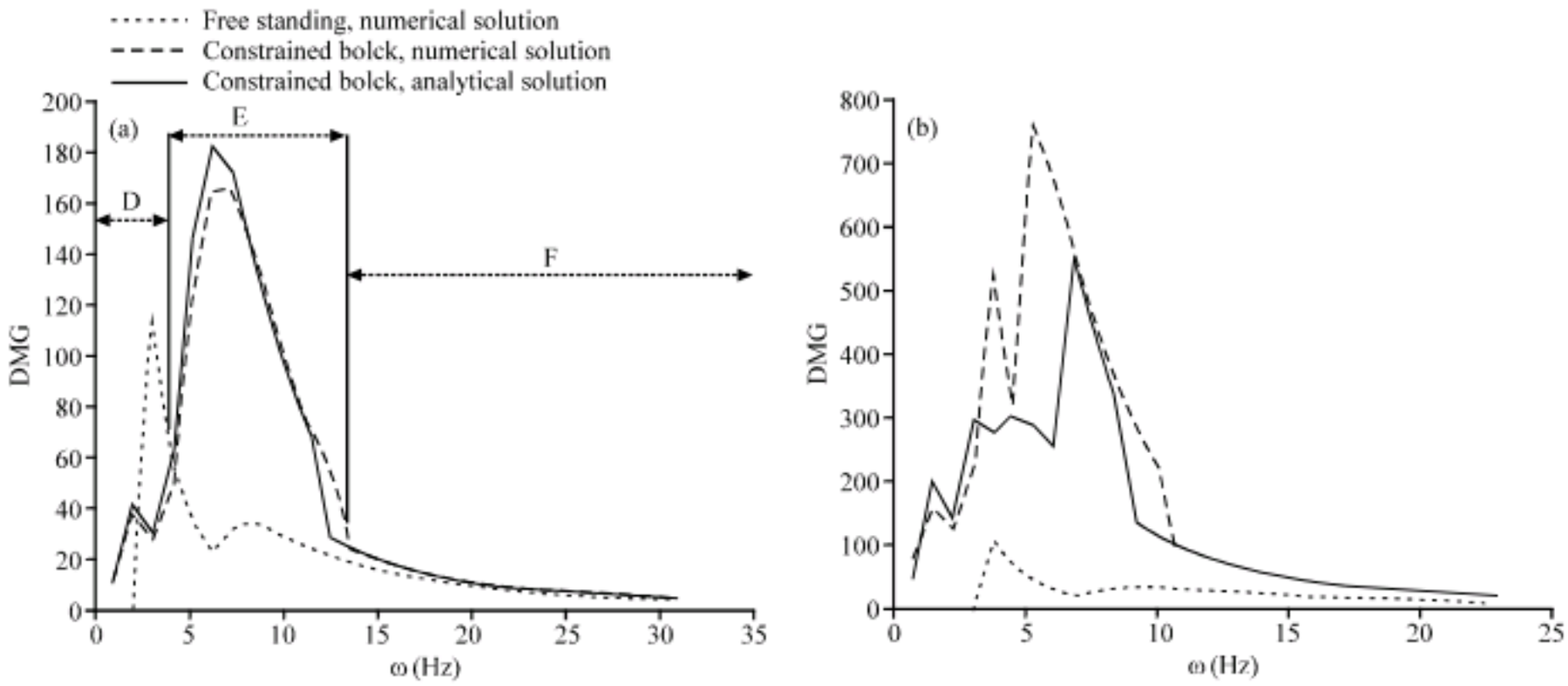

Fig. 15: Damage index (a) case study No.1 and (b) case study No.2 according to Table 3

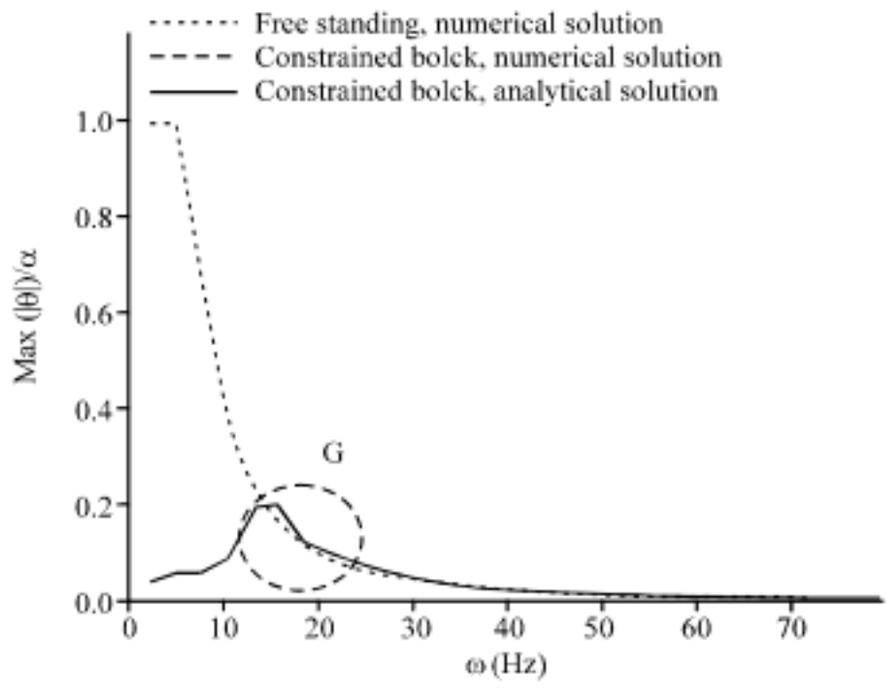

Fig. 16: Maximum normalized rocking response, case study No. 3 according to Table 3

response. The best efficiency of the link element in reducing the block rotation is in short frequency excitations (frequency range which is marked as A and D in Fig. 14a and 15a, respectively). In this range of frequency, the rocking rotation and damage index are lower than free-standing state. It means that block rotation and damage index have been beneficially reduced. In middle frequencies (usually in a range of $\omega>2q$) as have been marked as B and E in Fig. 14a and 15a, respectively, the link element does not have noticeable reducing effects on the block rotation but can increase the damage index. This means that worst case in efficiency of the link element is middle frequencies. In high frequencies (usually in the range of $\omega>2q$) as have been marked as C and F in Fig. 14b and 15a, respectively, the link element does not have noticeable effects on the block rotation and damage index. Comparison of Fig. 14a and b which are for same block but with different mass (case study No.1 and 2) shows that with increasing the mass of block, the maximum normalized rotation nears to the free-standing state. By increasing the mass of block, the interaction parameter of kh^2/I near to zero and can be vanished from the response formulations. In all case studies, an acceptable compatibility between numerical and analytical methods in calculation of maximum rotation can be observed. Figure 15b shows some discrepancies between numerical and analytical results in calculation of damage index.

CONCLUSION

In this study, dynamic behavior of a constrained rocking block as the representative of constrained rigid equipment has been studied. The exact governing equations and simplified analytical rocking formulation also have been introduced. The derived analytical solution later is verified with numerical solution of the exact governing equation and results showed acceptable accuracy between two methods. Derived analytical formulations showed that by interning of the link element, four sets of rocking response formulation may be formed. In the response space of a constrained block, appearance of some new patterns such as build-up like and beating-like response is probable that these patterns are new in comparison with the response of a free-standing rigid block. Constraining of a rigid equipment to a supporting structure can reduce the rocking rotation of the equipment in a wide range of base excitation frequency but in return can increase the amount of damped energy due to the contacts of the block to the base in some input frequencies. This can be known as a risk potential for the equipments which have leakage potential or have weak wedges.

REFERENCES

Allen, R.H. and X. Duan, 1995. Effects of linearization on rocking block toppling. J. Struct. Eng., 121: 1146-1149.

Anagnos, T., 2001. Development of an Electrical Substation Equipment Performance Database For Evaluation of Equipment Fragilities. Report No. PEER 2001/06, Pacific Earthquake Engineering Research Center, University of California, Berkeley.

Apostolou, M., G. Gazetas and E. Garini, 2007. Seismic response of slender rigid structures with foundation uplifting. Soil Dynamics Earthquake Eng., 27: 642-654.

Aslam, M., W.G. Godden and D.T. Scalise, 1980. Earthquake rocking response of rigid bodies. J. Eng. Mech. Div., 106: 377-392.

Bathe, K.J., 1996. Finite Element Procedures. 1st Edn., Prentice Hall Inc. Englewood Cliffs, New Jersey, ISBN: 0-13-301458-4, pp: 735.

Bernal, D., 1991. Locating event in step-by-step integration of equations of motion. J. Struct. Eng., 117: 530-545.

Boroschek, R. and A. Iruretagoyena, 2006. Controlled overturning of an unanchored rigid, bodies. Earthquake Eng. Struct. Dynamic, 35: 695-711.

Der-Kiureghian, A., 1999. Interaction in Interconnected Electrical Substation Equipments Subjected to Earthquake Ground Motions. Pacific earthquake Engineering Research Center, University of California, Berkeley.

Hogan, S.J., 1990. The many steady state responses of a rigid block under harmonic forcing. Earthquake Eng. Struct. Dynamic, 19: 1057-1071.

Hogan, S.J., 1994. Slender rigid block motion. J. Eng. Mech., 120: 11-24.

Hogan, S.J., 2000. Damping in rigid block dynamics contained between side-walls. Chaos Solitons Fractals, 11: 495-506.

Housner, G.W., 1963. The behavior of inverted pendulum structures during Earthquakes. Bull. Seismological Soc. Am., 53: 404-417.

Ishiyama, Y., 1982. Motions of rigid bodies and criteria for overturning by earthquakes. Earthquake Eng. Struct. Dynamic, 10: 635-650.

Jeong, M., K. Suzuki and S.C.S. Yim, 2003. Chaotic rocking behavior of freestanding objects with sliding motion. J. Sound Vibration, 262: 1091-1112.

Mahin, S.A. and J. Lin, 1983. Construction of Inelastic Response Spectra for Single Degree of Freedom Systems, Report No. UCB/EERC-83/17, Earthquake Engineering Research Center. 1st Edn., University of California at Berkeley, Berkeley, California.

Makris, N. and J. Zhang, 1999. Rocking Response and Overturning of Anchored Equipment Under Seismic Excitations. Report No. PEER 1999/06, Pacific Earthquake Engineering Research Center, University of California, Berkeley.

Makris, N. and Y.S. Roussos, 2000. Rocking response of rocking blocks under near-source ground motion. Geotechnique, 50: 243-262.

Nau, J.M., 1983. Computation of inelastic spectra. J. Eng. Mech. Div., 109: 279-288.

Peña, F., F. Prieto, P.B. Lourenco, A. Campus Costa and J.V. Lemos, 2007. On the dynamics of rocking motion of single rigid structures. Earthquake Eng. Struct. Dynamic, 36: 2383-2399.

Psycharis, I.N., 1981. Dynamic Behaviour of rocking structures allowed uplifting. Report No. EERL-81-02, California Institute of Technology.

Shenton, H.W. and N.P. Jones, 1991a. Base excitation of rigid block bodies, I: Formulation. J. Eng. Mech., 117: 2286-2306.

Shenton, H.W. and N.P. Jones, 1991b. Base excitation of rigid block bodies, II: Periodic slide-rock response. J. Eng. Mech., 117: 2307-2328.

Singh, M.P., L.M. Mreschi, L.E. Suarez and E.E. Matheu, 2006. Seismic design forces I: Rigid non-structural components. J. Struct. Eng., 132: 1524-1532.

Spanos, P.D. and A.S. Koh, 1984. Rocking of rigid blocks due to harmonic shaking. J. Eng. Mech. Div., 110: 1627-1642.

Tso, W.K. and C.M. Wong, 1989. Steady state rocking response of rigid blocks Part 1: Analysis. Earthquake Eng. Struc. Dynamic, 18: 89-106.

Wong, C.M. and W.K. Tso, 1989. Steady state rocking response of rigid blocks Part 2: Experiment. Earthquake Eng. Struct. Dynamic, 18: 107-120.

Yang, Y.B., H.H. Hung and M.J. He, 2000. Sliding and rocking response of rigid blocks due to horizontal excitations. Struct. Eng. Mech., 9: 1-16.

Yim, C., A.K. Chopra and J. Penzien, 1980. Rocking response of rigid blocks to earthquakes. Earthquake Eng. Struct. Dynamic, 8: 565-587.

Yim, C. and H. Lin, 1991. Nonlinear Impact and chaotic response of slender rocking objects. J. Eng. Mech., 117: 2079-2100.